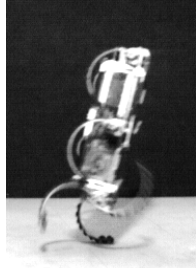


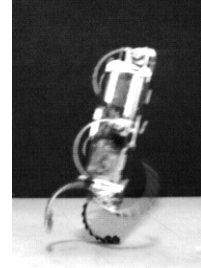
Towards bipedal running of a six-legged robot



N. Neville and M. Buehler

neville@cim.mcgill.ca, buehler@cim.mcgill.ca

Ambulatory Robotics Laboratory
Centre for Intelligent Machines, McGill University
Montreal, Quebec, H3A 2A7, Canada
www.cim.mcgill.ca/~arlweb, www.rhex.net



Abstract

This paper presents preliminary bipedal running experiments with our Robotic Hexapod, RHex. The robot and the bipedal gait are under-actuated, using only one actuated degree of freedom per compliant leg. We ‘doubled up’ the hind legs by attaching a duplicate set of hind legs at 180 degrees, forming ‘S’ shaped hind legs. This reduces the actuator speed requirements during non-contact, while preserving the bipedal dynamics and control challenges. Stable running at an average 1.08 m/s with a success rate of 59% (100% without steering failures) over ten runs is obtained with only leg angle and body pitch angle feedback. The average specific resistance (cost of transport) of 1.2 is lower than previously reported numbers for pronk and bound gaits at similar speeds.

1 Introduction

Many application domains of robots require mobility. Such applications include fire fighting, support for emergency first response teams, mobile monitoring, inspection and surveillance, planetary exploration, anti-terror and homeland security, to name just a few. To address these needs, engineers have designed a huge array of devices with wheels, tracks, and various numbers of legs, as well as articulated wheels and tracks, and combinations of legs and wheels. Of all these devices, legged robots resemble animals most. Thus, in addition to the potential for the kind of breathtaking mobility many animals are capable of, two more application domains exist for legged robots. First, entertainment robotic devices (toys, theme park versions of movie creatures) and robots designed to be human helpers require biological resemblance. Second, since legged robots must solve similar dynamic challenges in terms of legged mobility as humans and animals, but are much easier to study, they may serve as vehicles of scientific study to postulate or test hypotheses about animal or human locomotion.

Naturally, legged robots may also benefit from inspiration from millions of years of biological evolution. This is the case with RHex, a hexapod robot inspired by

research on cockroach locomotion [3,4] with its sprawled posture, low center of gravity, passive compliant legs, and clock-driven tripod gaits. These biologically motivated ideas, combined with sound scientific and engineering principles, have endowed RHex with a large repertoire of gaits, including walking over highly broken and irregular terrain [9], pronking [6], stair climbing [7,8], swimming [11], flipping [10] and quadrupedal bounding [2].



Figure 1: RHex in outdoor rock field

In this paper we introduce the first steps towards adding a new behavior to RHex’s already large behavioral repertoire: running on its hind legs. Just as the overall robot design was inspired by Full’s research on cockroach locomotion, so is this particular behavior. Full and Tu [4] reported that the American cockroach, *Periplaneta americana* (mass < 1 g) can run bipedally on its hind legs at high speeds. At the highest attainable speeds, the bipedal gait may even include an aerial phase (short periods with no measurable ground forces).

Why create a bipedal gait for a hexapod robot? We are interested in expanding RHex’s behavioral repertoire and investigating and exploiting possible mobility, speed or energetic advantages. For example, we expect an immediate mobility improvement in terms of step and pipe traversal heights, due to the raised center of mass of a bipedal RHex. Furthermore, the reported behavior is a proof of concept and an important step towards an unmodified bipedal RHex, which will be the simplest autonomous running biped, in terms of sensing, computation and mechanical design.

2 Platform

RHex is an untethered hexapod with a very simple mechanical design featuring compliant legs with one actuated degree of freedom per leg at the hip. Leg retraction is accomplished by rotating the leg over the hip to avoid toe stubbing and to clear obstacles. The simplicity of the system has resulted in a robust platform for studying legged locomotion that is also a promising candidate for many practical applications. Some key physical characteristics of RHex are given in Table 1, together with the diagram in Figure 2 showing RHex in upright running mode.

Body Mass	M_B	8.4 kg
Leg Mass	M_L	0.08 kg
Body Length	L_B	0.51 m
Body Height	H_B	0.14 m
Leg Length (unloaded)	L_L	0.17 m
Leg Spring Constant (linear approximation)	K_L	1700 N/m
Maximum Hip Torque (intermittent only)	τ_{\max}	5 Nm
Maximum Hip Speed	ω_{\max}	5 rev/s

Table 1: Basic RHex Data

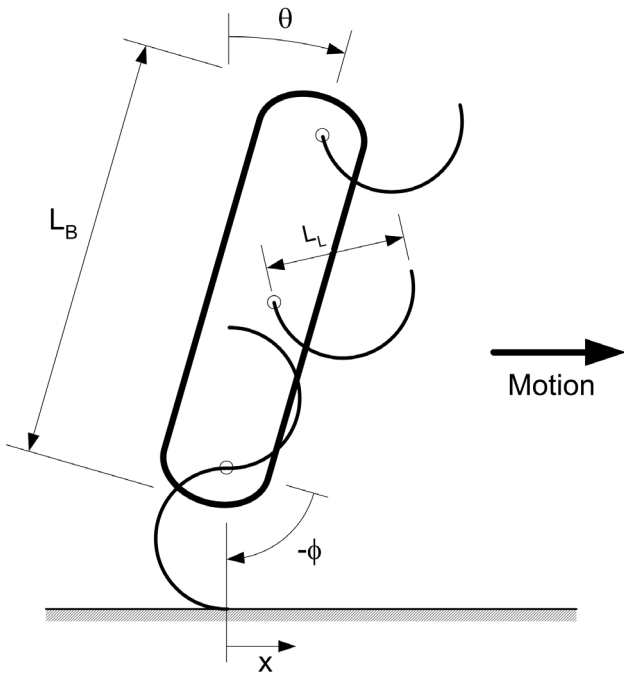


Figure 2: Biped running variables

For the basic hexapedal tripod gait, open loop target trajectories are shown in Figure 3, parameterized by four variables: the cycle time t_c , the stance time t_s , the stance angle ϕ_s , and the leg offset wrt the body, ϕ_0 . The duty factor t_s / t_c determines the “double support” duration, t_d , where both leg sets are in their slow phases, but possibly not all of them touching the ground. In a single cycle, both tripods go through their slow stance phase and fast swing phase, covering ϕ_s , and $2\pi - \phi_s$, respectively.

During bipedal running, the front four legs are not used. The rear two legs alternate in a similar fashion as the two tripod leg sets alternate in tripod gait, prescribed by the motion profiles in Figure 3. To maintain stable running, we continuously adjust the trajectories’ parameters, as described in the subsequent section.

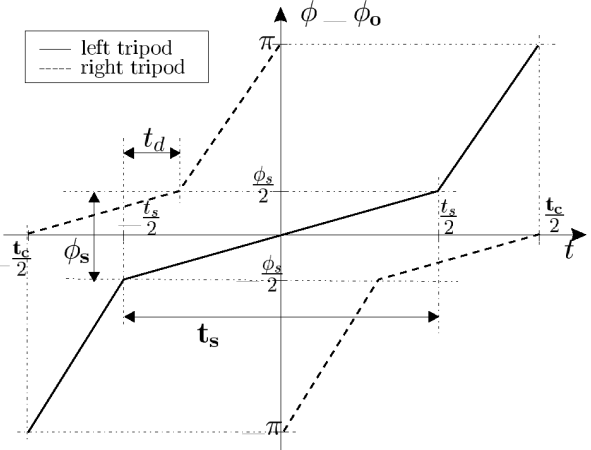


Figure 3: Motion profiles for left and right tripods for normal tripod gait

We modified the hind legs as follows: we attached an additional, identical half-circle shaped leg to each of the two hind legs, with a 180 deg offset, as shown in the diagram in Figure 2 and the photo in Figure 4. This “S” shape modification reduces the actuator speed requirements when not in stance, but otherwise does not fundamentally change the dynamics or control of the system. However, this change accommodates the current motor-gear speed capabilities and has facilitated this first bipedal operation. Any result reported here could be implemented with unmodified legs were higher leg speeds available. As we understand the dynamic and control better, and are able to operate at lower forward speeds, we plan to demonstrate bipedal operation without this leg modification.

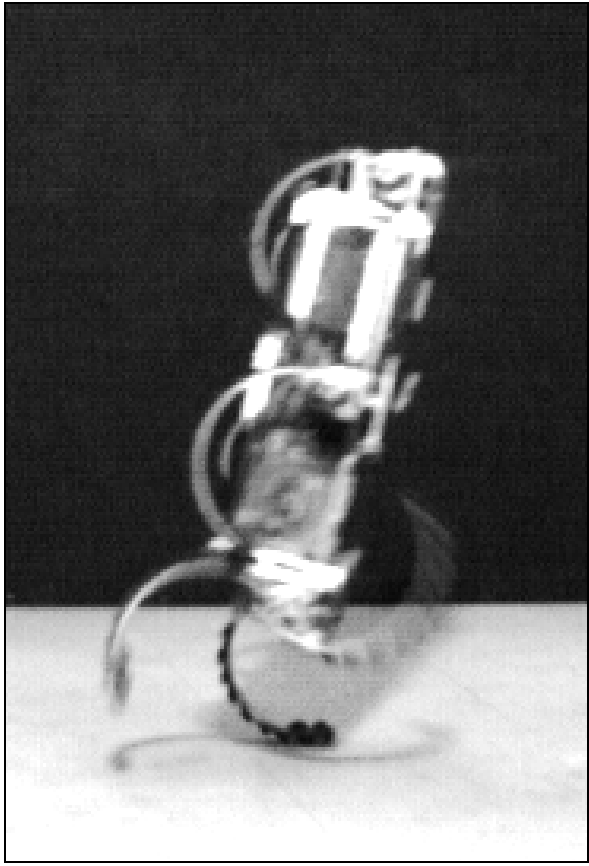


Figure 4: High speed still photo during single support phase in a 1 m/s bipedal run.

3 Sensing

The control strategy uses minimal feedback – leg angles wrt the body, $\phi_{l,r}$, and body pitch (lean) angle, θ . The two angles of the rear legs are measured by incremental optical encoders attached to the hip actuators. The body pitch angle is measured via integrating the pitch rate from a fiber optic laser gyro. The biggest sensing challenge is the absence of a forward velocity sensor. Instead we use a low pass filtered version of the desired leg velocities as an estimate of the actual forward velocity.

Actual forward velocity, body COM coordinates, leg lengths and angles after bending, leg forces, leg touchdown and liftoff events, are all not easily measurable and were not available. Body roll and yaw were available also from integrated gyro rate data, but as yet were not used for control.

4 Control

The controller is hierarchical, with three levels of PD controls for speed control, inverted pendulum balance

control and leg trajectory tracking. The elements of the overall block diagram in Figure 5 are described below.

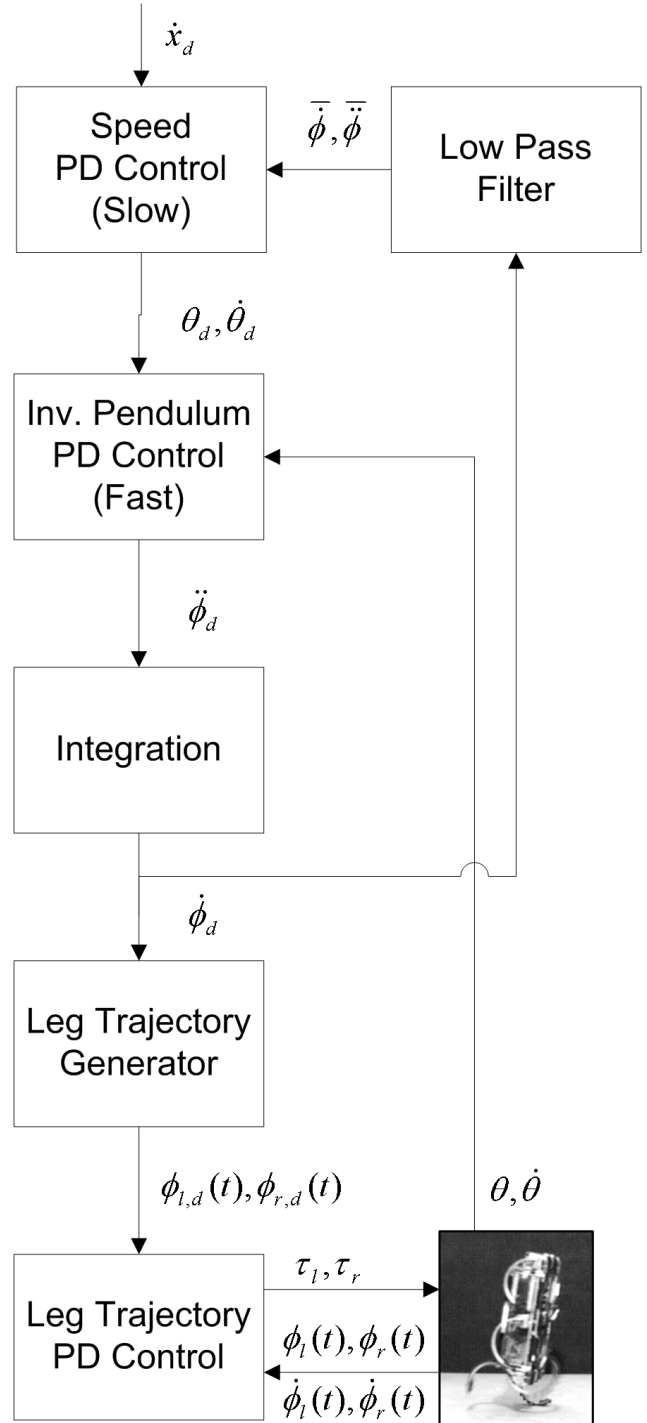


Figure 5: Control block diagram

Speed PD Control

The input to the speed control is the desired forward speed, \dot{x}_d , which is converted to a desired leg stance velocity via the effective average leg length during stance, $l_{leg} = 0.15\text{m}$. The PD controller

$$\theta_d = sat \left[k_{\phi p} \left(\bar{\phi} - \frac{\dot{x}_d}{l_{leg}} \right) + k_{\phi v} \ddot{\phi} \right] \quad (1)$$

generates desired pitch angles, θ_d , for the inverted pendulum PD balancing controller. We limit this term to +/- 3.5 degrees. Commanding positive pitch angles will increase the robot speed and vice versa. Since both speed and body pitch need to be controlled simultaneously, but only one control input to the robot is available via the desired leg speed, $\dot{\phi}_d$, the speed PD control is set such that it responds more slowly than the more important inverted pendulum balancing controller.

Inverted Pendulum PD Control

The robot balancing problem is equivalent to the inverted pendulum on cart problem. The linear PD control

$$\ddot{\phi}_d = k_{\phi p} (\theta - \theta_d - \theta_0) + k_{\phi v} (\dot{\theta} - \dot{\theta}_d) \quad (2)$$

is used in the pitch plane. It commands leg stance accelerations, $\ddot{\phi}_d$. A constant pitch offset angle, θ_0 , captures the difference between the pitch angle where the robot is balanced and vertical. $\dot{\theta}_d$ is calculated online as the derivative of the desired pitch angle commands from the Speed PD Control, θ_d .

Integration

The desired leg stance speed is obtained via integration of the desired leg stance acceleration and the current leg stance speed estimate, via

$$\dot{\phi}_d = \bar{\phi} + \ddot{\phi}_d dt. \quad (3)$$

Leg Trajectory Generator

Four leg trajectory parameters are used: ϕ_0 , ϕ_s , $\dot{\phi}_d$, and df . These are directly related to the four standard tripod trajectory parameters mentioned previously. The sweep angle, ϕ_s , is set to be a linear function of the desired stance velocity, $\dot{\phi}_d$. The offset is a function of the

pitch of the robot, $\phi_0 = \theta + C_1$, where C_1 is a constant.

Together, the sweep angle and offset determine the angle of the legs when the assumed touchdown and liftoff events occur. The fraction of the cycle that double leg support is assumed is given by $(2 \cdot df - 1)$. Here, the duty factor is calculated so that a desired constant single leg support time is achieved. The duration of single leg support is a key factor that determines the roll oscillation amplitude.

The clock driven leg trajectories are updated in a 1 kHz (nominal) control loop. The commanded leg positions and velocities are based on a normalized time, which maps a cycle period onto the unit interval. The cycle period is given by

$$t_c = \frac{\phi_s}{\dot{\phi}_d \cdot df}. \quad (4)$$

Four phases are created based on the normalized time. In the case of a constant sweep velocity command there is a stance phase, followed by a standard three part trapezoidal velocity profile as shown in Figure 6. The constant high velocity phase is characterized by the maximum leg velocity and exists only when the leg trajectory requires it. The trajectory parameters are updated during each sampling period. The resulting trajectories are smooth by virtue of the fact that the rate at which the trajectories are recalculated is sufficiently high. The two legs are kept 180° out of phase by having the cycle time offset of 0.5 between the legs.

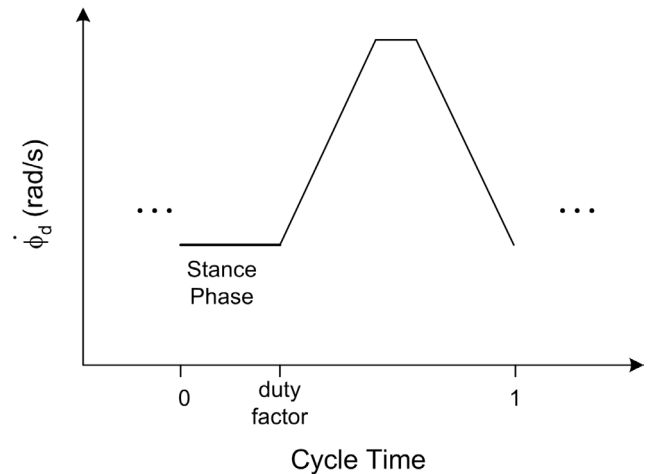


Figure 6: Leg trajectories for a constant sweep velocity command

Leg Trajectory PD Control

The desired left and right leg trajectories are tracked with a PD controller during stance and flight phases.

Low Pass Filter

The leg velocities during stance are estimated by simply passing the desired leg velocities through a 0.75 s low pass filter,

$$\bar{\dot{\phi}}_{d,k} = \alpha \dot{\phi}_d + (1 - \alpha) \dot{\phi}_{d,k-1}, \quad (5)$$

and the accelerations are the first order difference of the leg velocity estimates:

$$\ddot{\bar{\phi}}_d = \frac{(\bar{\dot{\phi}}_{d,k} - \bar{\dot{\phi}}_{d,k-1})}{dt}. \quad (6)$$

Roll

The main failure mode currently is roll instability. For relatively small disturbances a (passively) stable small amplitude rolling oscillation is present. Larger disturbances can cause the rolling oscillations to amplify until failure. A small roll amplitude is obtained by controlling the time that the robot is supported by only one leg. Stability in the roll plane was primarily addressed by appropriate duty factor values and by choosing appropriate leg trajectory tracking gains.

Actuator Saturation

Another major limitation in performance is actuation saturation in the retraction phase where high leg velocities are required. In order to facilitate controller tuning two legs were attached 180° apart on each hip. In this way the distance the leg has to rotate in retraction was reduced. Once the controller stability and speed range is optimized “double legs” will be removed. Since we are only limited in speed, but not torque, a different gear selection could help solve this shortcoming.

5 Experiments

Method

The robot is run repeatedly on a standard linoleum floor over a 4 m distance which is demarcated by start and end reflective tape. The robot is started manually in upright posture at a distance of approximately 2 m before the start tape. The robot senses the start and end tapes via a mounted IR (infrared) sensor and stores the traversal time for average speed calculation. The width of the hallway is 2 m, and the robot is started in the middle.

If the robot veers off to hit the wall (more than 1 m lateral travel) before the 4 m distance is traversed, this event is noted as a steering failure, since active steering control has not yet been implemented. The effect of the variation in distance traveled over the 4 m test track (a slight increase in actual average speed vs the quantity reported) is neglected. We repeat the runs until ten successful runs are obtained. A run where the robot traverses both the start and the end tape upright without touching the walls is counted as a successful run.

Results

We performed 17 successive runs, to obtain 10 successful runs. All 7 discounted runs were unsuccessful due to steering failures – the robot ran into the wall before completing the 4 m distance. Thus the success rate is 59% if we count the steering failures. None of the 17 runs failed due to speed or body pitch instabilities. Thus the success rate is 100% if we discard the steering failures. The mean velocity of the ten runs was 1.08 m/s with a standard deviation of 0.0247 m/s.

Figure 7 shows stable run data over a 5 s (approx. 5m) run. The top plot shows desired and actual body pitch angles, with pitch errors limited to +/- 2 degrees most of the time, with occasional +/- 4 degree error spikes. Roll angles (middle plot) remain limited to +/- 5 degrees. Leg stance speed data are relatively constant with an average error of about +/- 100 deg/s.

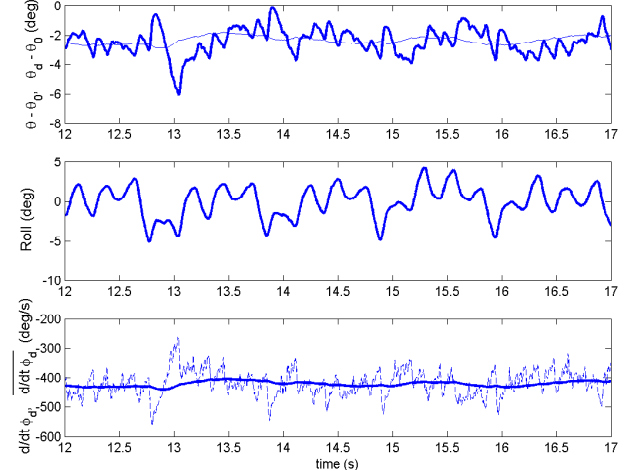


Figure 7: Typical pitch, roll and leg velocity plots during 1 m/s runs. Lighter lines indicate desired quantities ('d' subscripted values).

Figure 8 shows the desired and actual leg angles. The trajectories are offset by 90 degrees (and not by 180 degrees as the regular tripod gait in Figure 3) due to the S shape legs. The desired trajectories are not as simple and

smooth as in Figure 3 because the gait parameters are updated continuously to achieve stable biped running.

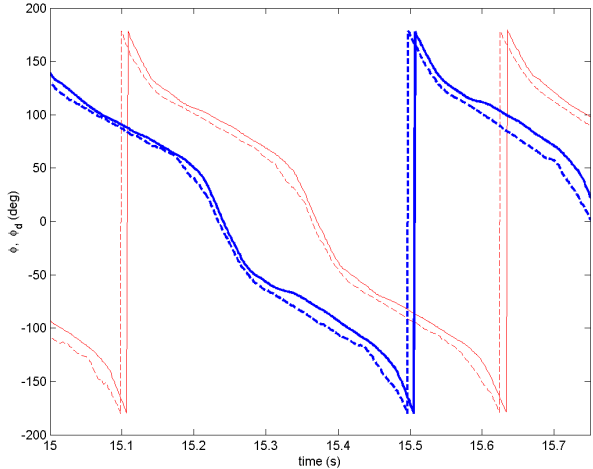


Figure 8: Desired (dash) and actual (solid) hind leg trajectories.

Figure 9 shows the corresponding desired and actual leg velocities (top plot) and the associated motor currents (bottom plot).

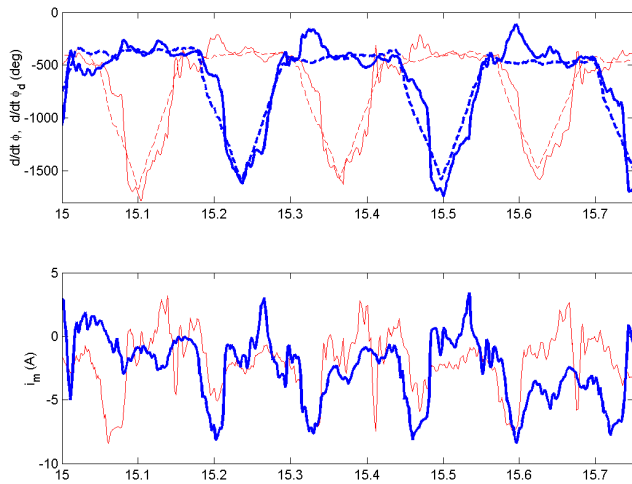


Figure 9: Top: typical desired (dash) and actual (solid) leg velocities. Bottom: motor currents. Darker/lighter lines differentiate left and right legs.

Energy efficiency is particularly important in power autonomous mobile robot applications. As a measure of energetic efficiency the specific resistance is used [5]. The measure of the energetic cost of locomotion is calculated as

$$\varepsilon = \frac{P}{m \cdot g \cdot v},$$

where P is the average total electrical power consumed, m is the mass of the robot, g is the gravitational constant, and v is the speed of locomotion. A sample instantaneous total electrical power during a 1 m/s run is shown in Figure 10. The power spikes occur around touchdown and liftoff where the moment due to gravity and inertia forces about the foot is largest. Over our ten runs it averages 107.31 W with a standard deviation of 3.428 W. This results in a specific resistance average of 1.20 with a standard deviation of 0.052. Figure 11 shows that this energetic performance compares very favorably with previously reported results.

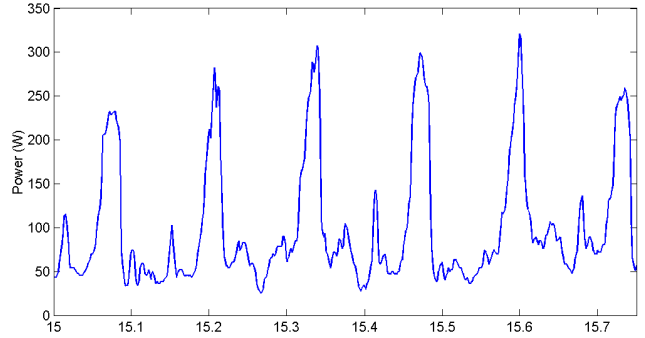


Figure 10 – Total electrical robot power consumption

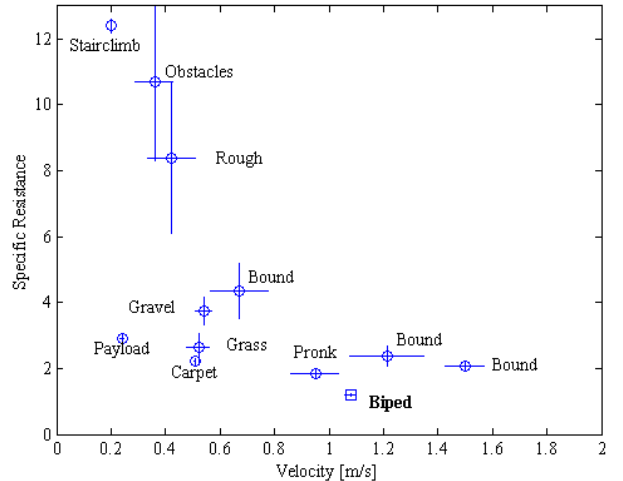


Figure 11 – Comparison of biped specific resistance with other RHex gaits.

Conclusion and Future Work

We have shown the first stable bipedal running of RHex, an autonomous, simple, one actuated DOF per leg hexapod, with S shape, compliant hind legs and minimal sensing. Encouraged by this initial success we are now

focusing on implementing RHex bipedalism with unchanged legs, implementing steering and yaw stabilization, further improving the speed range and stability through better modeling and control. In addition, we are developing behaviors that will permit RHex to stand up autonomously to transition from six to two legs.

Acknowledgements

This work was supported by DARPA/SPAWAR contract N66001-00-C-8026. The authors would like to thank the other RHex project's Principal Investigators and their local university teams for making this research possible, and for providing a stimulating and supportive research environment – Dr. D. E. Koditschek at University of Michigan, Dr. A. A. Rizzi at Carnegie Mellon University and in particular Dr. R. J. Full at University of California at Berkeley for providing the inspiration for RHex and its bipedal gait, and for many related fascinating discussions and tutorials about animal locomotion. Furthermore we gratefully acknowledge the help the team members at McGill's Ambulatory Lab, in particular to D. McMordie, M. Smith, C. Prahacs, and D. Campbell for help with various aspects of robot design, maintenance, sensing, logging or coding. N. Neville was supported by the Natural Sciences and Engineering Research Council of Canada (NSERC).

References

- [1] R. Blickhan and R.J. Full, "Similarity in multilegged locomotion: bouncing like a monopode", *J. Comparative Physiology*, vol. A. 173, p. 509-517, 1993.
- [2] D. Campbell and M. Buehler, "Preliminary Bounding Experiments in a Dynamic Hexapod", In B. Siciliano and P. Dario, eds, Experimental Robotics VIII, in "Lecture Notes in Control and Information Sciences", Springer-Verlag, p. 612-621, 2003.
- [3] R.J. Full, K. Autumn, J.I. Chung, and A. Ahn, "Rapid negotiation of rough terrain by the death-head cockroach", *American Zoologist*, vol. 38, p. 81A, 1998.
- [4] R.J. Full and M.S. Tu, "Mechanics of a rapid running insect: two-, four-, and six-legged locomotion." *J. exp Biology*, 156:215-231, 1991.
- [5] G. Gabrielli and TH. von Karman, "What Price Speed?", *Mechanical Engineering*, 775-781, Oct 1950.
- [6] D. McMordie and M. Buehler, "Towards Pronking with a Hexapod Robot," *4th Int. Conf. Climbing and Walking Robots*, p. 659-666, 2001.
- [7] E.Z. Moore and M. Buehler, "Stable Stair Climbing in a Simple Hexapod", *4th Int. Conf. Climbing and Walking Robots*, p. 603-610, 2001.
- [8] E.Z. Moore, D. Campbell, F. Grimminger and M. Buehler, "Reliable Stair Climbing in the Simple Hexapod 'RHex'", *IEEE Int. Conf. Robotics and Automation*, p. 2222-2227, 2002.
- [9] U. Saranli, M. Buehler and D.E. Koditschek, "RHex: A Simple and Highly Mobile Hexapod Robot," *Int. J. Robotics Research*, 20(7):616-631, July 2001.
- [10] U. Saranli and D.E. Koditschek, "Back flips with a hexapedal robot," *IEEE Int. Conf. Robotics and Automation*, p.2209-2215, 2002.
- [11] video of 1999 swimming implementation at www.cim.mcgill.ca/~arlweb and www.rhex.net